

Experimental investigation of early-time diffusion in the quantum kicked rotor using a Bose-Einstein condensate

G.J. Duffy[†], S. Parkins[‡], T. Müller[†], M. Sadgrove[‡], R. Leonhardt[‡], and A. C. Wilson[†]

[†] *Department of Physics, University of Otago, P.O. Box 56, Dunedin, New Zealand*

[‡] *Department of Physics, University of Auckland, Private Bag 92019, Auckland, New Zealand*

(Dated: November 23, 2018)

We report the experimental observation of resonances in the early-time momentum diffusion rates for the atom-optical delta-kicked rotor. In this work a Bose-Einstein condensate provides a source of ultra-cold atoms with an ultra-narrow initial momentum distribution, which is then subjected to periodic pulses (or “kicks”) using an intense far-detuned optical standing wave. A quantum resonance occurs when the momentum eigenstates accumulate the same phase between kicks leading to ballistic energy growth. Conversely, an anti-resonance is observed when the phase accumulated from successive kicks cancels and the system returns to its initial state. Our experimental results are compared with theoretical predictions.

I. INTRODUCTION

The delta-kicked rotor (DKR) is a nonlinear dynamical system which exhibits starkly contrasting behaviour in classical and quantum regimes. For example, the well-known chaotic diffusion exhibited by the classical DKR is completely suppressed by coherence effects (dynamical localization [1, 2]) in the quantum regime. The field of quantum chaos (see, e.g., [3, 4]), which brings together the study of classically chaotic systems and their quantum mechanical analogues, is relatively new, especially given the maturity of the two parent fields. Indeed, most of the progress in quantum chaos has been made only during the last quarter century.

From an experimental point of view, the field of quantum chaos received a major boost in the 1990’s with the use of ultra-cold atoms and pulsed standing-wave laser fields to realize a near-ideal quantum version of the delta-kicked rotor [5]. At the low temperatures achievable using laser cooling, quantum behavior of the atomic particles becomes manifest, and optical manipulation of the atoms offers unprecedented control over the forces they experience. Furthermore, one can identify for this system an “effective Planck’s constant”, \hbar , which is directly proportional to the period of the laser pulsing and can therefore be adjusted to, in a sense, make the system “more” or “less” quantum mechanical.

This so-called “atom-optical kicked rotor” has since been the subject of intense investigation by a number of experimental groups in a variety of different contexts (see, e.g., [6, 7, 8, 9, 10]). These investigations have in general focused on the long-time behavior of the system; that is, on the properties of the system after a relatively large number (at least several tens) of kicks. For these purposes, widths of the initial momentum distributions on the order of a few photon recoils (i.e., $\sigma_p \sim 4\hbar k_L$, where k_L is the wave number of the laser light) have sufficed, since the effects under investigation have typically not been dependent on starting from extremely precise initial states of the atomic motion. However, for detailed investigations of early-time behavior of the kicked rotor

and of certain uniquely quantum mechanical phenomena, it is extremely desirable, or even essential, to have yet more control over the initial state.

While most work on the kicked rotor has concentrated on differences between classical and quantum behavior in the late-time regime early-time behavior was investigated by Shepelyansky [11, 12]. This work showed that significant differences also exist in *initial* diffusion rates, and the initial quantum diffusion rate exhibits a strong dependence on the effective Planck’s constant \hbar . Also this dependence can also lead to signatures in the late-time energies [9, 10, 13] and diffusion rates [14, 15], but for a direct study of initial rates a very narrow initial momentum distribution is vital from the point of view of being able to resolve small energy changes as a function of the system parameters after just a small number of kicks. Furthermore, more recent theoretical work [16] has revealed that, with a very narrow initial momentum distribution, initial diffusion rates exhibit an even richer structure (as a function of \hbar) than that predicted by Shepelyansky, whose calculations assumed broad (uniform) initial conditions.

At certain specific values of \hbar – in particular, where \hbar is a rational multiple of 4π – quite remarkable phenomena can occur in the form of so-called “quantum resonances” and “anti-resonances” [16, 17, 18, 19, 20, 21]. These phenomena require particular initial momentum states which evolve in such a way that during the free evolution period in between kicks the different components of the state vector of the system experience either identical phase shifts, or a phase shift that alternates in sign from one momentum component to the next. Where the phase factor is identical for all components, ballistic energy growth is observed (quantum resonance). Where the phase factor alternates in sign, the system returns identically to its initial state after every second kick (quantum anti-resonance). With a broad initial momentum distribution such resonance and anti-resonance behavior can still be observed experimentally in the atom-optical kicked rotor [9, 21], but it is far less pronounced than in the ideal case of initial momentum eigenstates. With a dilute atomic Bose-Einstein condensate however, it is

possible to realize an initial state that is, to all intents and purposes, a momentum eigenstate and therefore allows a much clearer investigation of these phenomena.

In this work, we follow the suggestion of Daley and Parkins in Ref. [16] and investigate the early-time behavior of the atom-optical kicked rotor using a Bose-Einstein condensate to provide a very narrow and precise initial momentum state of the atoms. We focus on investigating the energy as a function of kick number for specific values of effective Planck's constant, and our results demonstrate the behaviors predicted theoretically. Note that our work complements recent experimental studies of atom-optical versions of (classically chaotic) nonlinear dynamical systems which also make use of extremely narrow atomic momentum distributions to provide very precise initial conditions [22, 23].

II. THE ATOM OPTICAL KICKED ROTOR

A. Theoretical Model

The basic model describing the atom-optical kicked rotor has been described by a number of authors, and here we briefly summarize this following the notation of Ref. [16]. A cold atomic sample interacts with a standing wave of laser light with frequency ω_L , far-detuned from resonance. The laser is pulsed with period T and pulse profile $f(t)$. Due to the large detuning, the internal atomic dynamics can be eliminated and the Hamiltonian determining the motion of the atoms can be written as

$$\hat{H} = \frac{\hat{p}^2}{2m} - \frac{\hbar\Omega_{\text{eff}}}{8} \cos(2k_L\hat{x}) \sum_{n=1}^N f(t - nT), \quad (1)$$

where \hat{x} and \hat{p} are the atomic position and momentum operators, respectively, and $\Omega_{\text{eff}} = \Omega^2/\delta$ is the effective potential strength, with $\Omega/2$ the (single-beam) resonant Rabi frequency and δ the detuning from atomic resonance. We can rewrite Eq. (1) as a scaled dimensionless Hamiltonian in the form

$$\hat{H}' = \frac{\hat{p}'^2}{2} - k \cos(\hat{\phi}) \sum_{n=1}^N f(t' - n), \quad (2)$$

which is standard for the kicked rotor system. The position operator is defined by $\hat{\phi} = 2k_L\hat{x}$, the momentum operator $\hat{p}' = 2k_L T \hat{p}/m$, the scaled time is $t' = t/T$, and $\hat{H}' = (4k_L^2 T^2/m) \hat{H}$. The classical stochasticity parameter (or kick strength) is given by $\kappa = \Omega_{\text{eff}}\omega_R T \tau_p$, where τ_p is the pulse length and $\omega_R = \hbar k_L^2/2m$ is the recoil frequency. In this work $f(t')$ is taken to represent a square pulse, i.e. $f(t') = 1$ for $0 < t' < \alpha$, where $\alpha = \tau_p/T$, in which case $k = \kappa/\alpha$. In these scaled units, we have $[\hat{\phi}, \hat{p}'] = i\bar{k}$, with $\bar{k} = 8\omega_R T$. Thus the quantum nature of the system is reflected by an effective Planck's constant, \bar{k} , which changes as we adjust the pulsing period T .

B. Early-time diffusion

In the case of the δ -kicked rotor (i.e., $\alpha \rightarrow 0$, $f(t') \rightarrow \delta(t')$) the evolution of the system can be represented by the quantized standard map,

$$\begin{aligned} \hat{\phi}_{n+1} &= \hat{\phi}_n + \hat{p}_n, \\ \hat{p}_{n+1} &= \hat{p}_n + \kappa \sin(\hat{\phi}_{n+1}), \end{aligned} \quad (3)$$

where $\hat{\phi}_n = \hat{\phi}(t' = n)$ and $\hat{p}_n = \hat{p}(t' = n)$, with the values recorded immediately after the kick at $t' = n$. In this version of the standard map, the first kick occurs at $t' = 1$.

In our experiment, an image of the atomic cloud allows us to determine the momentum distribution and hence the kinetic energy after a set number of kicks. With the change in kinetic energy between consecutive kicks we then determine the momentum diffusion rate

$$D(n) = \frac{\langle \hat{p}_n^2 \rangle}{2} - \frac{\langle \hat{p}_{n-1}^2 \rangle}{2}. \quad (5)$$

An analytical investigation of early-time quantum diffusion rates in the DKR was made by Shepelyansky [11, 12], whose calculations assumed uniform (broad) initial position and momentum distributions and involved the evaluation of quantum correlation functions of the form $\langle [\sin(\hat{\phi}_n), \sin(\hat{\phi}_0)]_+ \rangle$ for $n \leq 4$. From a sum of such correlation functions an estimate of the initial quantum diffusion rate was obtained, which predicts (broad) peaks, or resonances, as a function of \bar{k} . In particular, prominent peaks appear in the diffusion rate where \bar{k} is an integer multiple of 2π , together with other maxima whose number and positions (with respect to \bar{k}) vary with kick strength κ .

More recently, Daley and Parkins [16] re-examined the early-time diffusion rates for very narrow initial momentum distributions, as is appropriate to atom-optical experiments with Bose-Einstein condensates. They find an even more complex and interesting structure in the diffusion rates as a function of \bar{k} , as exemplified by their result for $D(2)$, which takes the form

$$\begin{aligned} D(2) &= \frac{\kappa^2}{4} [1 - J_2(K_{2q}) e^{-2\sigma_\rho^2} \cos(\bar{\rho}_0)] \\ &\quad - \kappa J_1(K_q) [\sigma_\rho^2 e^{-\sigma_\rho^2/2} \cos(\bar{\rho}_0) + \bar{\rho}_0 e^{-\sigma_\rho^2/2} \sin(\bar{\rho}_0)] \\ &\quad + \frac{\kappa^2}{2} [J_0(K_q) - J_2(K_q)] \cos(\bar{k}/2) e^{-\sigma_\rho^2/2} \cos(\bar{\rho}_0), \end{aligned} \quad (6)$$

where $K_q = 2\kappa \sin(\bar{k}/2)/\bar{k}$, $K_{2q} = 2\kappa \sin(\bar{k})/\bar{k}$, and a Gaussian initial momentum distribution of mean $\bar{\rho}_0$ and variance σ_ρ^2 is assumed. The rates $D(3, 4, 5)$ exhibit still more structure than for $D(2)$, but were computed numerically using wave function simulations [15, 16, 24] (which allow for finite pulse widths and atomic spontaneous emission). Note that for a broad initial momentum distribution $D(2)$ is independent of \bar{k} and given simply by $D(2) = D(1) = \kappa^2/4$.

C. Quantum resonances and anti-resonances

The phenomena of quantum resonances and anti-resonances occur for particular values of $\hbar k$, and in their “idealized” forms require very specific initial conditions. Take, for example, an initial momentum eigenstate $|\rho_0 = j\hbar k\rangle$, where j is an integer. Through the kicking process, this state couples only to eigenstates $|\rho = (j + j')\hbar k\rangle$, where j' is also an integer. If $\hbar k$ is an even multiple of 2π , then it is straightforward to show that $\exp(i\hat{p}^2/2\hbar k)|(j + j')\hbar k\rangle = |(j + j')\hbar k\rangle$, i.e., during the free evolution period in between kicks the state vector of the system is unchanged. This leads to ballistic energy growth (i.e., the energy depends quadratically on kick number) and dynamical localization does not occur. This is known as a quantum resonance and is related to the Talbot effect in wave optics [25]. In contrast, if $\hbar k$ is an odd multiple of 2π , then $\exp(i\hat{p}^2/2\hbar k)|(j + j')\hbar k\rangle = |(j + j')\hbar k\rangle$ if $j + j'$ is even, and $-|(j + j')\hbar k\rangle$ if $j + j'$ is odd. In this case, the system returns identically to its initial state, $|\rho_0 = j\hbar k\rangle$, after every second kick. This effect is known as a quantum anti-resonance.

Other features (i.e., peaks or dips) appearing in the diffusion rates as a function of $\hbar k$ (see Fig. 2) can also be related to behavior such as that described above. However, unlike quantum resonances and anti-resonances, the $\hbar k$ values for which these features occur depend on the kick strength κ in a nontrivial manner [16].

III. EXPERIMENT

We focus on the behavior of the energy as a function of kick number and of the effective Planck’s constant, $\hbar k$. The kick strength is fixed by keeping the laser intensity constant and varying both the pulsing period T (which is proportional to the effective Planck’s constant) and pulse length τ_p , such that the product $T\tau_p$ is a constant. The experiment is performed with a Bose condensate of approximately 10^4 ^{87}Rb atoms in the $F = 2$, $m_F = 2$ hyperfine state. The condensate is formed (as described in Ref. [26], but with minor modifications [27]) in a time-averaged orbiting potential trap with harmonic oscillation frequencies of $\omega_r/2\pi = 71$ Hz radially and $\omega_z/2\pi = 201$ Hz axially. After radio frequency evaporation to form a Bose condensate, the trap is relaxed to $\omega_r/2\pi = 32$ Hz and $\omega_z/2\pi = 91$ Hz over a period of 200 ms.

A. Kicking

Once formed, the condensate is released from the trap and exposed to pulsed optical standing waves after 1.7 ms of free expansion (so that condensate mean-field effects can essentially be ignored [28]). For our parameters, the momentum FWHM of the Bose condensate is $0.03 \times 2\hbar k_L$.

These standing waves are generated by two counterpropagating laser beams with parallel linear polarizations, derived from a single beam which is detuned 1.48 GHz from the $5S_{1/2}, F = 2 \rightarrow 5P_{3/2}, F' = 3$ transition. For a chosen κ value, the pulse period is scanned from $21.12 \mu\text{s}$ ($\hbar k = 4$) to the quantum resonance at $T = 66.38 \mu\text{s}$ ($\hbar k = 4\pi$). Consequently the pulse length is varied from $1.25 \mu\text{s}$ to 400 ns. There are limitations on the precise values of T and τ_p caused by the incremental stepsize values of the pulse generator. The laser detuning and intensity were chosen to give the desired kicking strength while maintaining a negligible spontaneous emission rate ($< 34 \text{ s}^{-1}$). The momentum distribution is determined using time-of-flight (4 ms of free expansion) and absorption imaging of the atomic sample. When the condensate is released from the magnetic trap it receives an (unwanted) impulse corresponding approximately to $12.5 \pm 0.5 \text{ mm/s}$, as determined by Bragg scattering [30]. In order to apply a standing wave which is stationary with respect to the condensate the frequency difference between the two laser beams is adjusted to remove the relative motion. A double-pass acoustic-optic modulator is used in each beam for altering its frequency and switching the optical potential on and off.

B. Energy measurements

The kicks given to the atomic sample populate momentum classes separated by $2\hbar k_L$ (as shown in Fig. 1). Following the kicks, we determined the kinetic energy of the atomic sample, which entailed counting the number of atoms in each momentum state and multiplying by the energy of that state. Subsequently, to obtain the average kinetic energy per atom this energy value was divided by $(2\hbar k_L)^2$ and the total number of atoms, and then multiplied by $m\hbar k^2$ (where m is the mass of the rubidium atom). This gave us an overall average energy in dimensionless units, $E = \langle \rho^2 \rangle / 2$.

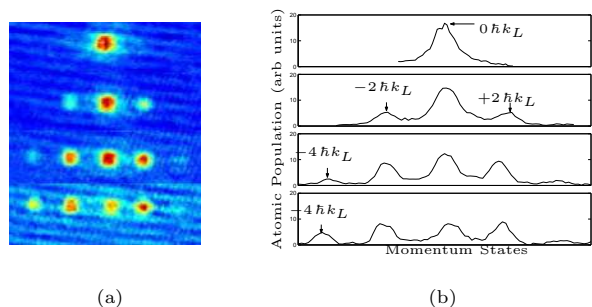


FIG. 1: (a) Typical time-of-flight images of atomic clouds separated in momentum by $2\hbar k_L$ for 1 (top) to 4 (bottom) kicks (b) Corresponding momentum distributions. This particular case illustrates enhanced energy growth close to the quantum resonance at $\hbar k = 4\pi$.

IV. EXPERIMENTAL RESULTS

We begin by highlighting the rich initial diffusion behavior of our kicked rotor system with experimental data for the energy after one and two kicks, $E(1)$ and $E(2)$, as a function of the effective Planck's constant, \hbar , for a fixed value of the kicking strength κ . This data, plotted in Fig. 2, confirms the prediction Ref. [16] of a uniform value for $D(1) = E(1) - E(0)$, but a strong dependence of $D(2) = E(2) - E(1)$ on \hbar , given a sufficiently narrow initial momentum distribution. Similar behavior is obtained for the higher kicking strength, as we shall see later.

The energy after one kick is given theoretically by $E(1) = \kappa^2/4$, which allows us to infer a value $\kappa = 7.7 \pm 0.6$ (11.7 ± 2) from the experimental data for the lower (higher) kicking strength. These values are consistent with those calculated from the laser intensity, detuning and pulse details. Note that for the one-kick data the duration of the kicking pulse was chosen for each \hbar value to match that used for sequences of two or more kicks, so the one-kick energies do in fact correspond to different experimental conditions. However, in dimensionless units the energy after one kick ($\langle \rho_1^2 \rangle / 2$) is predicted to be constant as a function of \hbar .

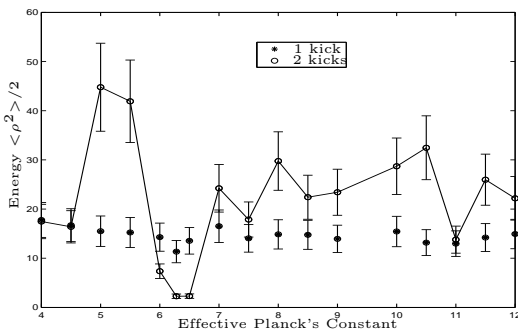


FIG. 2: Experimental energies (in dimensionless units) after 1 and 2 kicks, $E(1)$ and $E(2)$, at the lower kicking strength. After 1 kick the energies are approximately constant as a function of the effective Planck's constant \hbar (theory predicts $E(1) = \kappa^2/4$, a constant). For a broad initial momentum distribution, theory predicts simply that $E(2) = 2E(1) = \kappa^2/2$, but for a very narrow initial momentum distribution the energy $E(2)$ is heavily dependent on \hbar and exhibits pronounced peaks and dips. The error bars reflect shot-to-shot variation in the atom number and fluctuation in the laser intensity.

Before continuing, we note that a related experiment in which a released Bose-Einstein condensate of sodium atoms was subjected to a sequence of two standing-wave laser pulses separated by a varying time delay was recently reported by Deng *et al.* [29]. While effects related to those displayed above could be inferred from their results, their work was not set in the context of the quantum kicked rotor – if one does so, then the experiment they performed corresponds to varying \hbar and κ simultaneously (since both parameters are proportional to the

kicking period T , and the laser intensity and τ_p were fixed for their measurements).

A. Energy versus kick number

The energy as a function of kick number exhibits a complex variety of behaviors as the effective Planck's constant is varied (for fixed κ). Examples are plotted in Figs. 3 and 4, where experimental energies for up to four kicks are shown. Close to $\hbar = 2\pi$ (Figs. 3(a) and 4(a)) one observes the anti-resonance phenomenon described earlier, in which the system returns (approximately) to its initial state after every second kick – this manifests itself as an oscillation in the energy. In contrast, near $\hbar = 4\pi$ (Figs. 3(c) and 4(c)) one sees a continual growth in the energy as a consequence of the phenomenon of quantum resonance. For the lower kicking strength, we also observe behavior suggesting a period-4 anti-resonance close to $\hbar = 10.5$ (Fig. 3(b)). Numerical simulations confirm this behavior, for $\kappa = 7$, at a value of \hbar in this vicinity. For the larger kicking strength similar behavior occurs to a certain extent, but is most pronounced at slightly larger values of \hbar . Unfortunately, falling signal-to-noise and the effects of a finite initial mean momentum means that it is very difficult to extract useful energy values beyond about 4 kicks and hence to rigorously confirm this higher-order behavior (at least with the experimental setup that was used).

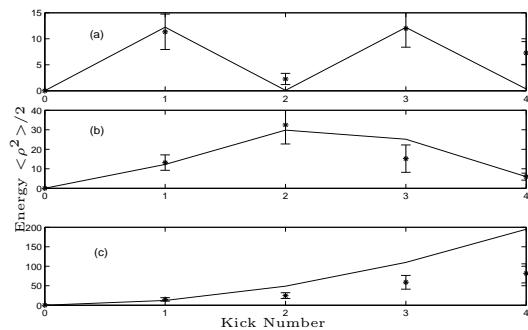


FIG. 3: Energy versus kick number for the lower kicking strength $\kappa = 7.7$ (a) $\hbar = 6.211$, (b) $\hbar = 10.523$, and (c) $\hbar = 12.573$. Crosses are experimental data, while the solid lines are the results of numerical simulations with $\kappa = 7$. Plot (a) illustrates anti-resonance behavior at $\hbar \simeq 2\pi$, while plot (b) demonstrates the presence of a period-4 anti-resonance close to $\hbar = 10.5$. Plot (c) illustrates enhanced energy growth close to the quantum resonance at $\hbar = 4\pi$.

Also plotted in Figs. 3 and 4 are the results of numerical simulations for the appropriate values of \hbar and α , and for $\kappa = 7.0$ and $\kappa = 11.7$, respectively. Quantitative agreement between theory and experiment is reasonably good, but notable deviations appear after several kicks for the anti-resonance and resonance at $\hbar \simeq 2\pi$ and 4π , respectively. We believe that these deviations are due

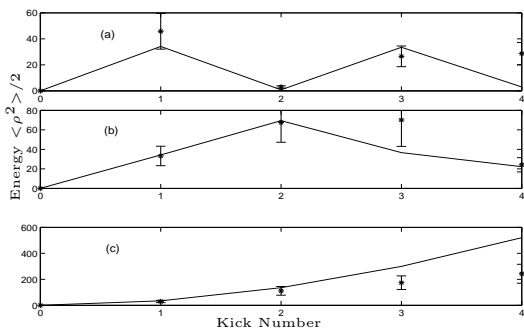


FIG. 4: Energy versus kick number for the higher kicking strength, $\kappa = 11.7$ (a) $\tilde{k} = 6.211$, (b) $\tilde{k} = 10.992$, and (c) $\tilde{k} = 12.573$. Similar resonance type behavior is observed in figure 3 as expected.

partly to fluctuations in the initial mean momentum of the atomic cloud relative to the laser standing wave. Inspection of the images of the kicked atomic clouds reveals that the position of the “zero momentum” peak can fluctuate from shot-to-shot by an amount of up to a few tenths of an atomic recoil. This was confirmed by Bragg scattering measurements [30] and is associated with the precise details of the switching-off of the time-averaged orbiting potential trap used to confine the initial Bose-Einstein condensate. As shown in [16], the quantum anti-resonance and resonance phenomena are particularly sensitive to any non-zero initial mean momentum of the atomic ensemble. In Fig. 5 we demonstrate this sensitivity with simulations for the parameters associated with Figs. 3(a) and 3(c), but now for initial mean momenta $\bar{p}_0 = 0.1 \hbar k_L$ and $\bar{p}_0 = 0.15 \hbar k_L$. The width of the initial momentum distribution is the same as in the experiment. As shown, with a finite value of \bar{p}_0 , one finds behavior more consistent with the experimental data.

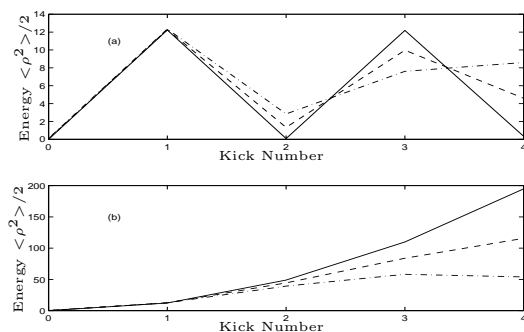


FIG. 5: Numerical simulations of energy as a function of kick number for (a) $\tilde{k} = 6.211$ and (b) $\tilde{k} = 12.573$, with $\kappa = 7$ and $\bar{p}_0 = 0$ (solid), $\bar{p}_0 = 0.1 \hbar k_L$ (dashed), and $\bar{p}_0 = 0.15 \hbar k_L$ (dot-dashed). The quantum anti-resonance and resonance phenomena are clearly very sensitive to the initial mean momentum of the atomic cloud.

The sensitivity of the energy to the initial mean momentum of the atomic cloud adds an extra variable to

the problem, over which we at present have little control. To further emphasize the dependence of the energy on the initial mean momentum, in Fig. 6 we plot the energy after two kicks, $E(2)$, using the theoretical result of Eq. (6) for several values of the initial mean momentum, \bar{p}_0 . This plot highlights the extreme sensitivity to initial motion of the quantum resonance at $\tilde{k} = 4\pi$, which in fact changes to an *anti-resonance* when $\bar{p}_0 = 0.5 \hbar k_L$. It follows that, in order to see resonance and antiresonance behavior controllably in their clearest forms, one requires very precise control over the initial mean motion of the atomic cloud.

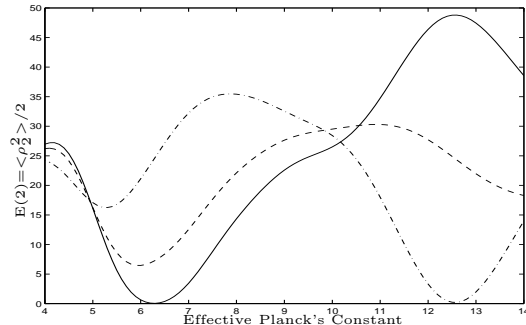


FIG. 6: Theoretical predictions using Eq. (6) for the energy after 2 kicks, $E(2)$, versus effective Planck’s constant \tilde{k} , for $\kappa = 7$ and $\bar{p}_0 = 0$ (solid), $\bar{p}_0 = 0.25 \hbar k_L$ (dashed), and $\bar{p}_0 = 0.5 \hbar k_L$ (dot-dashed). These results further illustrate the sensitivity of the energy growth rate to the initial mean momentum of the atomic cloud, particularly at the quantum resonance ($\tilde{k} = 4\pi$).

V. CONCLUSION

In summary our results show a rich structure of resonances as a function of the effective Planck’s constant and kick number for the atom-optical kicked rotor with a narrow initial momentum distribution. For two kicks we have shown that the resonant behavior is a more complex than those predicted by Shepelyansky for a system with a broad initial momentum distribution. Moreover we observed quantum anti-resonance ($\tilde{k} = 2\pi$) and quantum resonance ($\tilde{k} = 4\pi$) in the energy as a function of \tilde{k} for different kick strengths. Comparison between theory and experiment showed reasonable agreement, but by introducing an initial mean momentum to the numerical model better agreement could be obtained. Consequently, we have shown that the quantum features are very sensitive to precise initial conditions. One possible method of eliminating the initial mean momentum of the condensate would be to perform the measurements with the condensate still confined by the magnetic trap. One difficulty with this is that for our apparatus, condensate micro-motion will be introduced [30]. In addition, mean field effects will occur, although the nonlinearity asso-

ciated with these provide an opportunity to investigate instability of the condensate wave function [31].

Fund of the Royal Society of New Zealand through grants 02UOO910 and UOA016.

Acknowledgments

The authors thank A. Daley for help with initial calculations. We acknowledge the support of the Marsden

-
- [1] G. Casati, B. V. Chirikov, F. M. Izrailev and J. Ford, in *Stochastic Behaviour in Classical and Quantum Hamiltonian Systems*, Vol. 93 of *Lecture Notes in Physics*, edited by G. Casati and J. Ford (Springer-Verlag, Berlin, 1979).
- [2] B. V. Chirikov, F. M. Izrailev and D. L. Shepelyansky, *Sov. Sci. Rev. C* **2**, 209 (1981).
- [3] L. Reichl, *The Transition to Chaos in Conservative Classical Systems: Quantum Manifestations* (Springer-Verlag, New York, 1992).
- [4] F. Haake, *Quantum Signatures of Chaos* (Springer-Verlag, New York, 1991).
- [5] F. L. Moore, J. C. Robinson, C. F. Bharucha, B. Sundaram, and M. G. Raizen, *Phys. Rev. Lett.* **75**, 4598 (1995).
- [6] M. G. Raizen, *Adv. At. Mol. Opt. Phys.* **41**, 43 (1999).
- [7] H. Ammann, R. Gray, I. Shvarchuck and N. Christensen, *Phys. Rev. Lett.* **80**, 4111 (1998).
- [8] J. Ringot, P. Szriftgiser, J. C. Garreau, and D. Delande, *Phys. Rev. Lett.* **85**, 2741 (2000).
- [9] M. B. d'Arcy, R. M. Godun, M. K. Oberthaler, D. Cassettari and G. S. Summy, *Phys. Rev. Lett.* **87**, 074102 (2001).
- [10] M. E. K. Williams, M. P. Sadgrove, A. J. Daley, R. N. C. Gray, S. M. Tan, A. S. Parkins, N. Christensen, and R. Leonhardt, *J. Opt. B: Quantum Semiclass. Opt.* **6**, 28 (2004).
- [11] D. L. Shepelyansky, *Theor. Math. Phys.* **49**, 925 (1982).
- [12] D. L. Shepelyansky, *Physica D* **28**, 103 (1987).
- [13] B. G. Klappauf, W. H. Oskay, D. A. Steck, and M. G. Raizen, *Phys. Rev. Lett.* **81**, 4044 (1998).
- [14] T. Bhattacharya, S. Habib, K. Jacobs, and K. Shizume, *Phys. Rev. A* **65**, 032115 (2002).
- [15] A. J. Daley, A. S. Parkins, R. Leonhardt, and S. M. Tan, *Phys. Rev. E* **65**, 035201(R) (2002).
- [16] A. J. Daley and A. S. Parkins, *Phys. Rev. E* **66**, 056210 (2002).
- [17] F. M. Izrailev and D. L. Shepelyansky, *Sov. Phys. Dokl.* **24**, 996 (1979).
- [18] F. M. Izrailev and D. L. Shepelyansky, *Theor. Math. Phys.* **43**, 553 (1980).
- [19] G. Casati and I Guarneri, *Commun. Math. Phys.* **95**, 121 (1984).
- [20] V. V. Sokolov, O. V. Zhirov, D. Alonso, and G. Casati, *Phys. Rev. Lett.* **84**, 3566 (2000).
- [21] W. H. Oskay, D. A. Steck, V. Milner, B. G. Klappauf, and M. G. Raizen, *Opt. Commun.* **179**, 137 (2000).
- [22] W. K. Hensinger, H. Häffner, A. Browaeys, N. R. Heckenberg, K. Helmerson, C. McKenzie, G. J. Milburn, W. D. Phillips, S. L. Rolston, H. Rubinsztein-Dunlop, and B. Upcroft, *Nature* **412**, 52 (2001).
- [23] D. A. Steck, W. H. Oskay, and M. G. Raizen, *Science* **293**, 274 (2001).
- [24] A. C. Doherty, K. M. D. Vant, G. H. Ball, N. Christensen, and R. Leonhardt, *J. Opt. B: Quantum Semiclass. Opt.* **2**, 605 (2000).
- [25] M. Berry and E. Bodenschatz, *J. Mod. Opt.* **46**, 349 (1999).
- [26] J. L. Martin, C. McKenzie, N. R. Thomas, J. C. Sharpe, D. M. Warrington, P. J. Manson, W. J. Sandle, and A. C. Wilson, *J. Phys. B: At. Mol. Opt. Phys.* **32**, 3065 (1999).
- [27] A.S. Mellish, G. Duffy, C. Mc Kenzie, R. Geursen and A.C. Wilson, *Phys. Rev. A.*, **68**, 051601(R) (2003).
- [28] J. Stenger, S. Inouye, A. P. Chikkatur, D. M. Stamper-Kurn, D. E. Pritchard, and W. Ketterle, *Phys. Rev. Lett.* **82**, 4569 (1999).
- [29] L. Deng, E. W. Hagley, J. Denschlag, J. E. Simsarian, M. Edwards, C. W. Clark, K. Helmerson, S. L. Rolston, and W. D Phillips, *Phys. Rev. Lett.* **83**, 5407 (1999).
- [30] R. Geursen, N. R. Thomas and A. C. Wilson, *Phys. Rev. A*, **68**, 043611 (2003).
- [31] C. Zhang, J. Liu, M. G. Raizen and Q. Niu, *Phys. Rev. Lett.* **92**, 054101 (2004).